

Article

Design and Experiment of an Internet of Things-Based Wireless System for Farmland Soil Information Monitoring

Guanting Ou ¹, Yu Chen ¹, Yunlei Han ², Yunuo Sun ¹, Shunan Zheng ^{3,*} and Ruijun Ma ^{1,*}

¹ College of Engineering, South China Agricultural University, Guangzhou 510642, China; ouguanting@stu.scau.edu.cn (G.O.); chenyu219@126.com (Y.C.); synnys1001@gmail.com (Y.S.)

² China Association of Agricultural Science Societies, Beijing 100000, China; hanyunlei@126.com

³ Rural Energy and Environment Agency, Ministry of Agriculture and Rural Affairs, Beijing 100000, China

* Correspondence: zhengshunan1234@163.com (S.Z.); maruijun_mrj@163.com (R.M.)

Abstract: Soil environmental monitoring is crucial for ensuring the sustainability and productivity of agriculture. This study aims to develop a wireless soil monitoring system that utilizes Narrowband Internet of Things (NB-IoT), solar energy, and Global Positioning System (GPS) technologies to address the issues of high labor demand, high costs, and delayed feedback in traditional soil monitoring methods. This system can collect soil temperature, humidity, and meteorological data in real time, transmit them to a cloud platform for analysis and visualization, and predict future soil data. It employs multiple learning algorithms to build models and uses the Tree-structured Parzen Estimator (TPE) algorithm for hyperparameter optimization. Field stability experiments were conducted on the system, and the performance of the soil moisture prediction model was evaluated. During the 84-day stability experiment, the system operated stably for 80 days, with a data collection success rate of 95.87%. In the performance evaluation of the soil moisture model, the GBDT model achieved a coefficient of determination (R^2) of 0.9838 on the validation set and a root-mean-square error (RMSE) of 0.0013, with an RMSE of 0.0013 on the test set as well. The experimental results demonstrate that the system is stable and reliable, featuring low power consumption, wide coverage, and high accuracy. It can effectively predict soil moisture, providing timely and accurate support for irrigation and farming decisions.



Academic Editor: Ivan Francisco

Garcia Tejero

Received: 10 January 2025

Revised: 21 January 2025

Accepted: 27 January 2025

Published: 21 February 2025

Citation: Ou, G.; Chen, Y.; Han, Y.; Sun, Y.; Zheng, S.; Ma, R. Design and Experiment of an Internet of Things-Based Wireless System for Farmland Soil Information Monitoring. *Agriculture* **2025**, *15*, 467.

<https://doi.org/10.3390/agriculture15050467>

Copyright: © 2025 by the authors. Licensee MDPI, Basel, Switzerland. This article is an open access article distributed under the terms and conditions of the Creative Commons Attribution (CC BY) license (<https://creativecommons.org/licenses/by/4.0/>).

1. Introduction

Monitoring parameters related to agriculture constitute a crucial link in agricultural production management. In farming management, the real-time acquisition of these parameters, which include soil moisture, soil temperature, air temperature, humidity, rainfall, and solar radiation, is of vital importance for analyzing drought and flood disasters and formulating management decisions [1]. Additionally, precise analysis of agrometeorological and weather parameters can assist farmers in optimizing tillage decisions and enhancing crop yields [2]. With the support of these data, farmers can choose appropriate pesticides and fertilizers more effectively, thereby further enhancing the growth quality of crops [3,4]. Therefore, researchers have developed farmland planting decision support systems to offer farmers expert guidance on agricultural activities and crop management [5,6]. These technologies, otherwise referred to as precision agriculture, have the capacity to minimize input costs and endow farmers with the ability to achieve higher crop yields [7].

Traditional methods for monitoring soil information typically depend on extensive field sampling and costly laboratory analyses. However, such laboratory analyses often

lack sufficient spatial and temporal resolution, making it challenging to dynamically track essential soil physical properties. Furthermore, these methods are inadequate for supporting high-precision agricultural management decisions [8]. To address these limitations, advanced sensing techniques, such as Frequency Domain Reflectometry (FDR) and Time Domain Reflectometry (TDR); precise sensor technologies; and remote sensing technologies have been developed to improve the accuracy of soil moisture monitoring [9]. These technologies provide higher precision and real-time data collection, offering better support for agricultural management decisions. In the past, establishing network connections in remote areas was challenging due to the high costs associated with high-quality sensors and inadequate network signal coverage. However, these issues are gradually being addressed [10]. With the development of microelectronics technology, lightweight communication protocols, open-source servers, and visualization tools, the Internet of Things (IoT) has become an effective solution for remote wireless monitoring [11–13] and has been applied in many fields. In addition, with the continuous development of environmental sensor and data logger technology, continuous data acquisition has become possible, providing strong support for agricultural management decisions [14]. Through the field deployment of the IoT and sensor technology, it is possible to achieve the real-time acquisition and wireless transmission of high-precision soil data, the effect of which is comparable to laboratory analysis, while significantly saving manpower.

In agricultural monitoring, Wireless Sensor Networks (WSNs) and Internet of Things (IoT) technologies are widely used for soil monitoring due to their low cost, high fidelity, and rapid deployment [15]. However, traditional wireless communication technologies, such as ZigBee and Wi-Fi, have certain limitations. ZigBee, while suitable for short-range and low-speed applications, has a limited communication range, making it appropriate only for small-scale networks. For example, Madhura et al. designed a ZigBee-based system for real-time soil quality monitoring, but its coverage was insufficient for large agricultural areas [16]. German et al. also designed a ZigBee-based system, but its ability to analyze hydrological processes was limited to small-scale farmlands [17]. Estrada-Lopez et al. designed a ZigBee-based intelligent soil parameter estimation system with dynamic power management, but the system's effectiveness was constrained by the same limitations of ZigBee [18]. Roy and Barman developed a ZigBee adaptive system for controlling and monitoring soil moisture and nutrients, but again, the short communication range of ZigBee limited its application in large-scale monitoring [19]. Additionally, ZigBee is vulnerable to environmental interference, limiting its effectiveness in complex agricultural environments. Wi-Fi, although used in remote monitoring systems such as Vieira et al.'s long-distance Wi-Fi-based monitoring platform, suffers from high power consumption and limited transmission range, making it unsuitable for large-scale agricultural monitoring [20]. Kuang et al. designed a farmland monitoring system based on a Wi-Fi cloud platform for comprehensive environmental parameter management, but the system was constrained by Wi-Fi's high power consumption and limited range, making it less effective for large-scale agricultural applications [21]. In contrast to ZigBee and Wi-Fi, LoRaWAN offers advantages in long-distance transmission and low power consumption. However, its low bandwidth restricts it to low-speed data transmission, making it less suitable for applications requiring high-frequency or large data transfers [22]. To overcome these limitations, NB-IoT (Narrowband IoT) emerges as a promising wireless communication technology. Unlike ZigBee, Wi-Fi, and LoRaWAN, NB-IoT offers lower power consumption, wider coverage, and lower communication costs, making it especially suitable for large-scale agricultural IoT applications. It operates in an authorized frequency band, reducing interference, and enables long-range data transmission without the need for relay nodes, which is particularly advantageous for rural and remote areas [23,24].

The Global Positioning System (GPS) provides crucial coordinate information for land topography analysis and agricultural environment monitoring [25]. In large-scale soil monitoring, the geographical location of each monitoring system is vital for spatial analysis. Although previous research has used multi-positioning sensor networks for certain monitoring scenarios, the GPS still holds an advantage in terms of accuracy, particularly in outdoor agricultural environments [26]. Many existing systems rely on separate GPS units or other positioning methods, often increasing hardware costs and complicating integration. In contrast, this study integrates the GPS module directly with the NB-IoT module in the soil monitoring system. This integration eliminates the need for additional hardware, streamlining the design and reducing costs while maintaining the high accuracy and reliability of GPS positioning. The continuous geolocation provided by the integrated GPS module ensures precise tracking of each monitoring point, even when the system is relocated, such as during the planting or harvesting seasons or when modifications are made to the field layout (e.g., new irrigation installations). This innovative integration not only improves the efficiency and accuracy of data acquisition but also leverages NB-IoT's fast communication protocol to ensure consistent data transmission with a low error rate. The combination of the GPS and NB-IoT offers a cost-effective solution while significantly enhancing the real-time performance of agricultural environmental monitoring. This approach represents an improvement over traditional methods by reducing hardware complexity and cost while ensuring high-quality, accurate data collection, especially in dynamic agricultural environments [27].

Wireless Sensor Networks (WSNs) and IoT-based systems have become key technologies for agricultural monitoring, providing real-time data on environmental parameters to improve decision making. Jangam et al. used Arduino to develop an agricultural meteorological system based on the IoT [2] that is equipped with a variety of sensors, such as temperature, humidity, and soil moisture sensors, and uses the GPRS module to connect to the Internet and send sensor data to the network server for further analysis. However, the system needs to be fixed in a specific location to continuously monitor the impact of crop growth, so the system is not easy to move, and the scope of application is limited to small farmland. Sawant et al. developed Sense-Tube [28], an agrometeorological monitoring system. The system obtains ambient temperature and humidity and soil temperature and humidity data through raspberry kits, connects to the base station through the Wi-Fi network for data collection, and uses web-based tools for data analysis. The system is powered by solar energy and has a battery as a backup power source. However, the system is not mobile, and it is costly to analyze weather–crop interactions. Ramadan et al. designed a wireless monitoring system for soil moisture content using an IoT kit [29]. Solar panels and two detectors (A and B) are connected to the IoT kit. Probes A and B are used to determine soil moisture at two different levels, using Frequency Domain Analysis (FDA) to analyze the data, and the analysis results are used to determine irrigation plans and agricultural activities. Mesas-Carrascosa et al. designed an agricultural environment monitoring system based on open-source hardware, which connects soil moisture and temperature sensors as well as air humidity and temperature sensors to the Arduino suite. The system can provide users with information for monitoring plant growth through the IoT toolkit and smart phone application [30].

The Internet of Things (IoT) has emerged as a critical network paradigm, enabling seamless interconnectivity among numerous smart devices that continuously generate vast amounts of data. With the rapid expansion of IoT applications and services, effectively analyzing and utilizing these data have become a key research focus. Meanwhile, machine learning, as a pivotal technology, has achieved remarkable success in fields such as computer vision, intelligent decision making, and control systems, providing powerful support

for the intelligent analysis and prediction of IoT data [31]. Shokati et al. [32] employed random forest (RF) models combined with Sentinel-2, Landsat-8/9, and UAV-based hyperspectral data to predict soil moisture, achieving high accuracy. However, their approach relies heavily on remote sensing data, which may pose challenges related to equipment costs and timely data acquisition. Wang et al. [33] explored various deep learning architectures for soil moisture prediction, emphasizing the effectiveness of long short-term memory (LSTM) networks in capturing temporal dependencies. Their study demonstrated that incorporating attention mechanisms and adversarial training improved feature extraction and prediction accuracy. However, the model's reliance on large, high-quality datasets and its computational complexity may limit its scalability and practical deployment in resource-constrained agricultural environments. These studies highlight the potential of machine learning techniques, particularly RF and LSTM, in improving the accuracy of soil moisture prediction. However, challenges related to data quality and adaptability to various application scenarios still require further investigation.

In conclusion, the IoT-based soil monitoring system not only enhances the efficiency of agricultural environmental monitoring but also provides robust scientific decision support for farmers, thereby promoting sustainable agricultural development. However, previous soil monitoring systems were often prohibitively expensive and overly complex, failing to meet the rapidly evolving demands for user-friendly interfaces, spatial query support, and flexible online/offline data collection modes. Consequently, these limitations led to relatively low accuracy in data acquisition. To address these challenges, this study designs and implements an advanced wireless soil monitoring system for farmland based on IoT technology. This system integrates NB-IoT wireless communication, GPS positioning modules, and high-precision sensors, effectively overcoming issues related to power consumption, long-distance transmission, and adaptability to complex environments. Compared with existing wireless communication technologies such as ZigBee, Wi-Fi, and LoRa, NB-IoT offers superior coverage, lower power consumption, and higher transmission stability, making it particularly suitable for large-scale agricultural applications. The integration of the GPS and NB-IoT not only improves geographic positioning accuracy but also simplifies hardware design, reduces system costs, and ensures efficient operation in dynamic agricultural settings. Furthermore, this study combines machine learning models with soil monitoring data to achieve accurate predictions of key agricultural parameters, such as soil moisture. This predictive capability significantly enhances farmers' ability to make informed decisions, especially in precision agriculture practices like irrigation and fertilization. The innovation of this research lies in its provision of a low-cost, high-precision, and scalable solution through system integration and technical optimization, offering a new perspective for agricultural environmental monitoring. The system's real-time data collection and long-term stable operation capabilities provide a reliable foundation for agricultural decision support systems, driving the advancement of agricultural production management towards intelligence and precision.

2. Design of System

2.1. Hardware System Design

2.1.1. Network Architecture of the Proposed System

The overall design of the system adopts the NB-IoT network architecture, as shown in Figure 1, and consists of an NB-IoT terminal, NB-IoT base station, NB-IoT packet core network, IoT connection management platform, and industry application server.

As one of the core communication technologies of the IoT, NB-IoT has become a key development field for domestic and foreign telecom operators due to its advantages of wide

coverage and low power consumption. The support for NB-IoT by operators such as China Unicom has provided a broad space for the development of agricultural IoT applications.

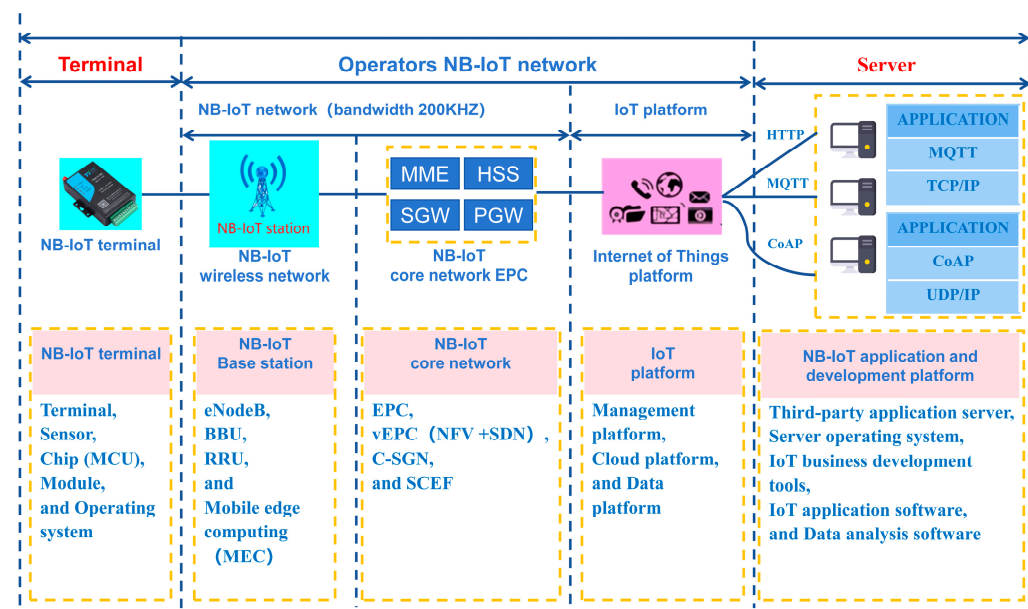


Figure 1. NB-IoT network architecture.

2.1.2. Soil Monitoring Sensor Unit

The soil monitoring sensor unit used in the hardware design of the system is mainly composed of a soil sensor, host microcontroller, NB-IoT wireless communication module integrated with the GPS, and a power management unit. The hardware structure of the soil monitoring sensor unit is shown in Figure 2. The hardware of the wireless soil monitoring system is shown in Figure 3. The hardware system is composed of integrated boxes and sensors, including a data logger (DL) with a built-in NB-IoT module and power module, solar panels, soil sensor, and weather sensor, with mobile function. Among them, the soil sensor is used to monitor the soil temperature and humidity, and the weather station contains a variety of meteorological sensors, which can measure the air temperature, relative humidity, wind speed, wind direction, rainfall, solar radiation, and other environmental parameters.

- (1) Sensors: The system uses TH30 soil sensors from TANGHUA ECOLOGY in Beijing, China. The TH30 sensor is capable of measuring the temperature, water content (VWC), and electrical conductivity of the soil. The TH30 sensor was calibrated at the factory, and its specifications are as follows: volume moisture content (VWC) range: 0~100%VWC; resolution: 0.08%VWC; accuracy: $\pm 1\text{--}3\%$; temperature range: $-40\text{--}80^\circ\text{C}$; resolution: 0.1°C ; accuracy: $\pm 0.5^\circ\text{C}$; conductivity range: 0~23 ds/m; resolution: 0.01 ds/m (0~7 ds/m) and 0.05 ds/m (7~23 ds/m); and accuracy: $\pm 5\%$ (0~7 ds/m). The probe material of the TH30 sensor is a special electrode for anti-corrosion, and the sealing material is black flame-retardant epoxy resin. It can operate normally in an environment of $-40\text{--}85^\circ\text{C}$, and the protection grade is IP68. It can be immersed in water for a long time. These features make the TH30 sensor very attractive for long-term soil health monitoring. The TH30 sensor draws power from the power management unit (3.6~12 V DC) and connects to the host microcontroller via the SDI-12. The TH30 sensor uses Frequency Domain Reflectometry (FDR) to detect soil moisture content. The probe of the sensor forms a capacitor, the steel needle/copper wire in the circuit board is the capacitor board, and the surrounding medium is the dielectric material, generating an electromagnetic field between the

positive and negative plates. The positive and negative electrodes of the capacitor form an LC oscillator circuit, and the frequency of the LC oscillator circuit is:

$$F = \frac{2\pi}{\sqrt{LC}}$$

where the oscillation frequency F changes as the inductance (L) and capacitance (C) change, the sensor uses a fixed inductance value, the change in oscillation frequency depends on the change in capacitance, and the change in capacitance is affected by the change in soil moisture. By measuring the frequency F , the dielectric constant ϵ is obtained, allowing the soil moisture content value to be obtained.

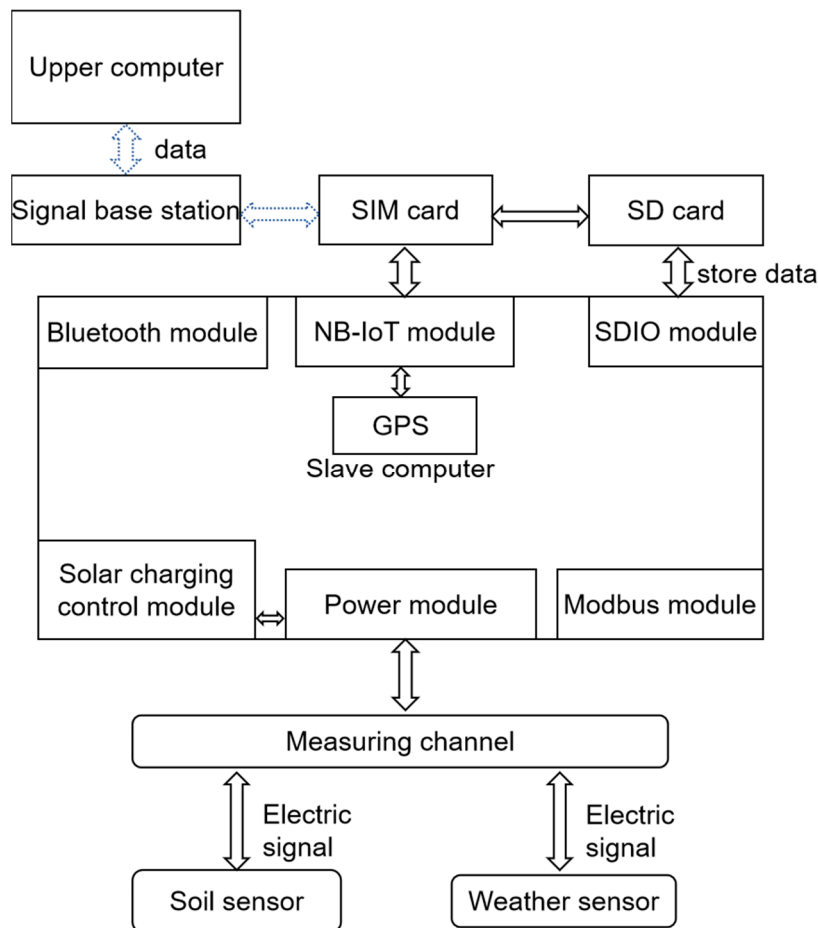


Figure 2. Hardware structure of soil monitoring sensor unit.

The meteorological sensors employed are the multi-element weather stations of the TH302 series, capable of detecting the air temperature, humidity, wind speed, wind direction, rainfall, and solar radiation.

- (2) Host microcontroller: The host controller is designed using the DL, which is responsible for controlling and coordinating all functions of the system. The DL is a highly integrated data logger with a built-in battery, charge controller, etc., and has an IP65 protective housing. In most cases, users only need to install solar panels to use it. The DL uses a waterproof aviation plug and optional junction box as the sensor connection port. The panel contains a switch, a Bluetooth wake button, a USB cable port, and five status indicators.

The measurement interface of the DL includes 5 analog channels, 1 switching channel, 1 frequency channel, 1 digital measurement channel of the SHT series temperature

and humidity sensor, 6 SDI-12 channels, and 1 RS485 channel, which can read SDI-12 sensor data and can use the MODBUS module to expand the measurement. This feature allows the user to improve the system independently and add new sensors to meet the working requirements.

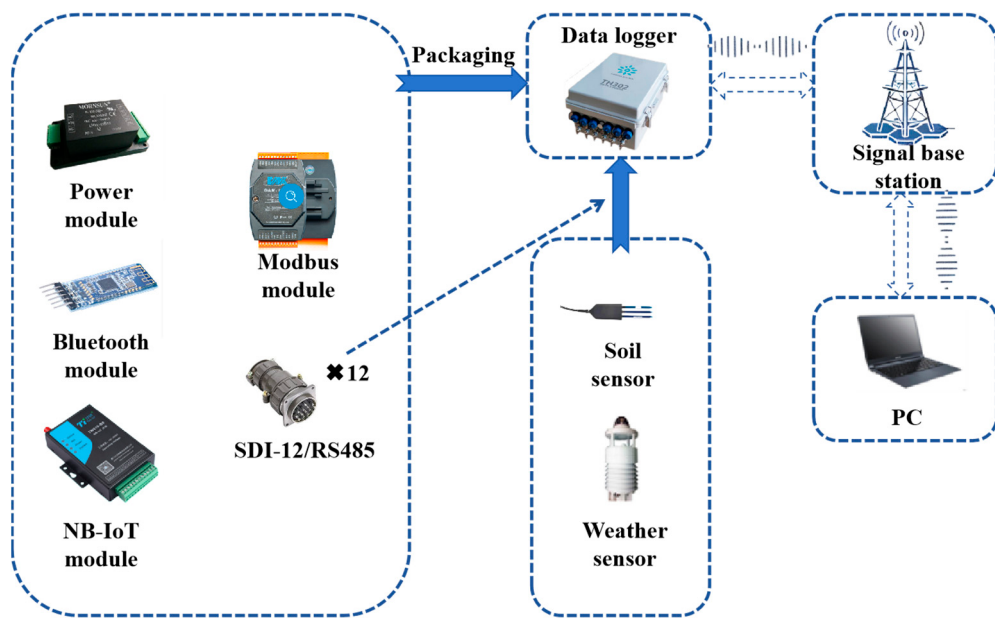


Figure 3. Physical diagram of soil wireless monitoring system hardware.

The DL supports 32 measurement variables, and each variable has 6 data values, including the real-time value, maximum value, minimum value, average value, period cumulative value, and permanent cumulative value, which are automatically calculated, stored, and sent according to the storage table.

The flow chart of measurement data acquisition by the master is shown in Figure 4. The process begins with periodic device wake-up, followed by the steps power supply, preheating, measurement, data storage, and data transmission, ultimately returning to a dormant state based on condition judgments and repeating the data collection task.

- (3) Wireless communications and GPS module: The DL can be connected to the mobile phone through Bluetooth, using the mobile phone app to set the parameters of the data logger, through the SIM card in the NB-IoT module. This not only provides the GPS positioning function but also realizes the remote transmission of data to the IoT platform. The login platform can be used to view and download data. The GPS-integrated NB-IoT wireless communication module has an embedded antenna, high sensitivity, and interference suppression capability.
- (4) Power management unit: The power management module includes the power supply channel and the solar charging controller. The built-in solar charging controller with an MPPT (Maximum Power Point Tracking) function, 20 Ah polymer lithium battery, and external solar panels effectively reduces the system operating costs.

The power channel refers to the interface used to supply power to the sensor during the measurement process. These channels are controlled by the collector and automatically opened and closed by the collector according to the user's settings. TH302 has 7 groups of controllable power channels, and the output voltages of these channels are 3.3 V and 12 V/5 V (others). These 6 power channels can be selected via a jumper to output 12 V or 5 V power supplies, which share a single power supply (battery) internally, so the number of channels open at the same time is limited by the maximum current that the power supply

can provide. In addition to these controllable power channels, the collector also provides a precision reference voltage source (VREF). The power supply is a normal output power supply and can only be used to provide a reference voltage source for the sensor; it cannot be used with a larger current sensor power supply.

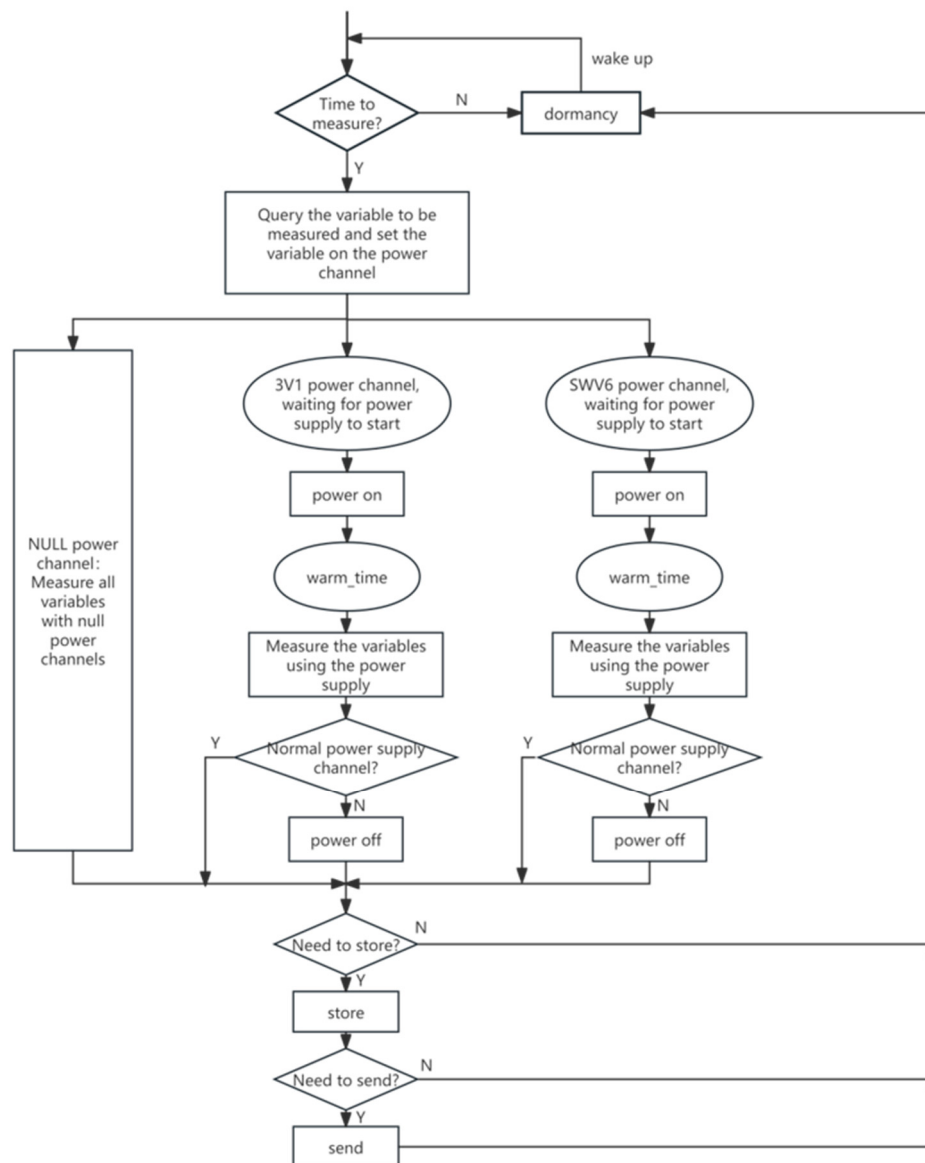


Figure 4. Flow chart of measurement data acquisition.

2.2. Software System Design

The software system utilizes a three-tier architecture comprising the presentation, application, and data layers. Each module supports functionalities such as interface interaction, data management, statistical analysis, visualization, and early warning. The architecture leverages a front-end stack (including Layui.js, Element UI, Node.js, and Echarts.js), a back-end stack (Spring Boot and Java Persistence API), and a MySQL database. These technologies enhance both development efficiency and system performance, ensuring a user-friendly interface, robust back-end operations, and smooth data interaction.

2.2.1. Performance Layer

The presentation layer functions as the system's front end, comprising the user interface. This research employs Layui.js, Element UI, Node.js, and Echarts.js for front-end

design and development. Node.js, built on the Chrome V8 engine, acts as the server environment, enhancing performance and simplifying development complexity. Layui.js, a modular and lightweight framework, performs effectively on server pages. Element UI provides a comprehensive library of components and templates for page design. Echarts.js, an open-source JavaScript library, facilitates the creation of interactive data visualization charts [34]. Ajax is used for dynamic web page updates by asynchronously exchanging small amounts of data with the server, enabling partial updates without reloading the entire page and streamlining data processing.

In the presentation layer of this system, the front-end user interface is developed using the Layui.js framework for data visualization. Components and templates from Element UI are integrated to enhance the interface esthetics and usability. Echarts.js is utilized to build and display the soil data visualization chart. The design monitoring system's data table interface is presented in Figure 5.



Figure 5. Data table interface of the monitoring system.

2.2.2. Application Layer

The application layer serves as the system's back end, encompassing the design and development of the framework, data access, and application support layers.

The back-end design adopts Spring Boot as the framework to deliver basic web development capabilities and a simplified configuration. As an open-source framework for Java applications, Spring Boot streamlines the development, deployment, and configuration [35]. It follows a convention-over-configuration approach, enabling developers to quickly set up and run standalone applications with default settings. Leveraging Spring Boot, the system facilitates rapid project construction, efficient data provisioning, and enhanced reliability and development efficiency.

The data access layer employs JPA (Java Persistence API) as an Object-Relational Mapping (ORM) tool to link data tables with entity classes for database manipulation. Through operations like adding, deleting, modifying, and querying entity classes, it simplifies MySQL database interaction and supports the addition, deletion, modification, and querying of soil data, along with interface paging functionality.

Finally, the application support layer adopts Baidu Map as the host of the map service and uses JavaScript API GL as the map development tool. Baidu Map JavaScript API GL is a set of application program interfaces written in JavaScript language, using WebGL to render maps, coverings, etc., and supporting a 3D view display map. It helps developers build rich and interactive map applications in websites and supports browser-based map application development on PC and mobile terminals. The designed system map service is shown in Figure 6.

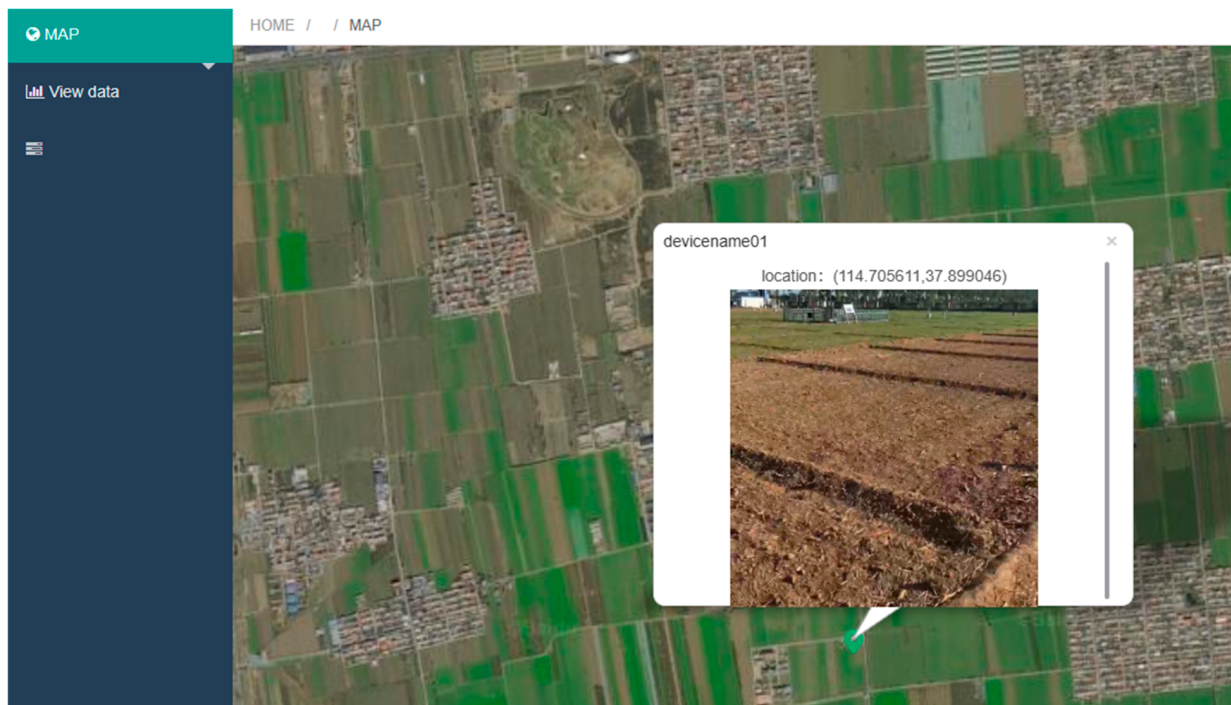


Figure 6. System map service.

2.2.3. Data Analysis Layer

The data analysis layer is mainly the design of machine learning models and databases.

Machine Learning Model

The object of machine learning is data, that is, starting from the data, extracting the features of the data, abstracting the data model, discovering the rules in the data, and then returning to the analysis and prediction of new data. This is shown in Figure 7.

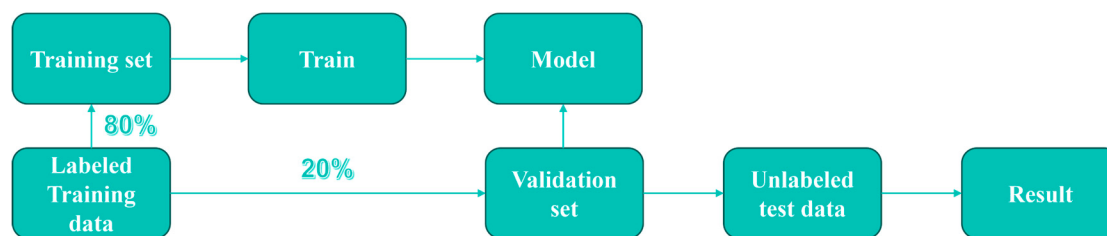


Figure 7. Machine learning process.

In this study, in the first step, machine learning methods such as linear regression, decision trees, random forest, long short-term memory (LSTM), and gradient boosting decision trees (GBDTs) are used to construct the prediction model of soil moisture.

Linear regression is a simple regression model used to explore the linear relationship between dependent and independent variables, which is easy to implement and interpret. Decision trees, which generate predictive models by recursively splitting feature spaces, are suitable for working with nonlinear data and are easy to understand but easy to overfit. Random forest is the integration of multiple decision trees to improve the prediction accuracy through majority voting or average results, with strong anti-noise and generalization capabilities. LSTM is a special type of recurrent neural network (RNN) that is suitable for processing and predicting data based on time series.

A GBDT is a boosting-based ensemble learning model that enhances prediction performance step by step. It effectively handles high-dimensional data and nonlinear relationships, excelling in data analysis and prediction. The algorithm employs categorical regression trees (CARTs) as weak learners and builds multiple weak learners iteratively using decision trees. A GBDT applies the gradient descent algorithm to train newly added weak classifiers by leveraging the negative gradient of the current model's loss function. The trained weak classifiers are integrated into the model to iteratively fit the loss function and optimize the overall model. The core formula of the GBDT algorithm is as follows:

First, the decision tree model is initialized (Equation (1)):

$$f_0(x) = \arg\min_c \sum_{i=1}^m L(y_i, c) \quad (1)$$

where $f_0(x)$ represents the initialized weak learner, and c is the optimal bias constant, minimizing the difference between this constant and the true dataset values. $L(y_i, c)$ denotes the loss function, capturing the error between the CART's predicted value and the actual target value. Each weak learner adjusts training samples based on the prior learner's performance and computes the residuals from the previous weak learner (Equation (2)).

$$R_{ki} = y_i - f_{k-1}(x_i), i = 1, 2, \dots, m \quad (2)$$

where f_{k-1} is the KTH weak learner.

Then, the residual r_{ki} is fit, a new weak learner $T_k(x)$ is created, and the learner is updated (Equation (3)).

$$f_k(x) = f_{k-1}(x) + T_k(x) \quad (3)$$

The above steps are repeated until the number of weak learners reaches the previously set hyperparameters. Finally, all the predictions of the weak learners are weighted and summed to form a strong learner that outputs the soil property predictions (Equation (4)).

$$f_{GBDT}(x) = f_0(x) + \sum_{k=1}^K T_k(x) \quad (4)$$

In the second step, the Tree Parzen Estimator (TPE) algorithm is applied to optimize model hyperparameters in the Python environment, ensuring high accuracy during training and prediction. The TPE algorithm, a single-objective Bayesian optimization method based on the Tree Parzen, addresses global optimization problems. It efficiently identifies the optimal hyperparameter configuration for machine learning models with minimal iterations, saving time. Using a Gaussian Mixture Model, the TPE algorithm models hyperparameters. During optimization, the hyperparameter set is split into two probability

density functions: $l(x)$, representing lower-risk hyperparameters, and $g(x)$, associated with higher-risk hyperparameters. The TPE formulas are defined in (5) and (6):

$$p(x|y) = \begin{cases} l(x) & \text{if } y < y^* \\ g(x) & \text{if } y \geq y^* \end{cases} \quad (5)$$

$$r = p(y < y^*) \quad (6)$$

where y^* denotes the threshold corresponding to the quantile r in the y set, with y^* ranging between (0,1) and a default r value of 0.15. The TPE uses expected improvement (EI) as the fetch function, calculated using the following equation:

$$EI_{y^*}(x) = \frac{ry * l(x) - l(x) \int_{-\infty}^{y^*} p(y) dy}{rl(x) - (1-r)g(x)} \propto \left(r + \frac{g(x)}{l(x)} (1-r) \right)^{-1} \quad (7)$$

where we can see that EI is proportional to $l(x)$ and inversely proportional to $g(x)$. $g(x)/l(x)$ is used to select the most appropriate x value so that the EI value is higher during the iteration. In each iteration, the algorithm returns x^* , the largest EI value, and participates in the next iteration. Finally, the optimal hyperparameter combination of the model is found.

(1) Database design

In this study, MySQL is used to design a database management system to store and manage user information, device information, variable information, and variable data. In the architecture of the MySQL database, the relationship between the user information table, device information table, variable information table, and variable data table is progressive, which is convenient for users to find data, and also protects the security of user information and data information. After successful login, the platform will find its device information according to the user table and display it in the platform, which is convenient for users to filter the device information to view the monitoring data of related devices. In addition to the basic device ID and device name, the device information table also includes the battery voltage, charging voltage, motherboard temperature, and atmospheric pressure of the device. The variable data table contains fields such as the primary key ID, variable ID, device ID, data value, and data time.

2.3. System Deployment and Testing

2.3.1. Deployment of the Developed System

The designed wireless soil monitoring system based on the IoT was deployed in an experimental field in Hebei Province of the Ministry of Agriculture and Rural Affairs. The arrangement of soil sensor TH30 is shown in Figure 8. Figure 8a shows the excavation of the soil profile according to the experimental design and the insertion of a total of 5 soil sensors at different depths (20–100 cm); Figure 8b shows that the sensor cable is exposed to the ground for about 1 m, and the remaining part is buried in the soil; Figure 8c shows that the vertical rod is inserted into the soil and that the data logger is fixed on the vertical rod with a throat hoop. Sensors installed at different depths of the soil allow more soil to be included in the measurement range, providing more comprehensive data on the soil environment. This configuration significantly improves the accuracy and representativeness of the data in soil monitoring, providing important support for an in-depth analysis of the soil profile characteristics.

After the system is deployed, online debugging is carried out as follows: First, turn on the Bluetooth function of the data logger, connect it with a smart phone, and use the installed Helper app (developed in Java under the Android Studio development environment,

released after debugging and testing). Search for the 8-bit unique identification code corresponding to the device and pair it. After entering the configuration interface, modify the channel, measurement, and storage settings according to the requirements, including the variable name and order of the measured values of each channel, as well as the server address for data reception, and set the frequency of data transmission, as shown in Figure 9 of the mobile app interface. The back end parses the raw data obtained from the server through the TCP protocol and stores the data to the corresponding device table in the database. Because the DL uses NB-IoT communication technology, it needs to insert a SIM card to use the network provided by the corresponding operator, which has the advantage of a simple layout compared with other communication technologies that require a gateway.

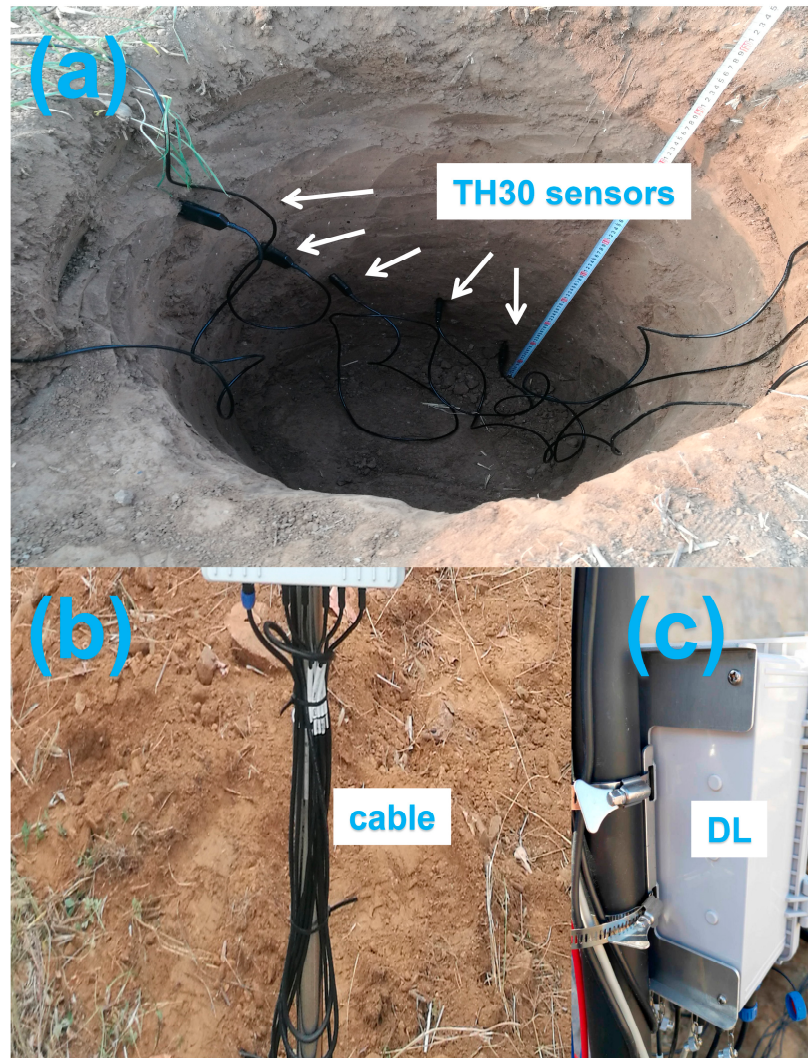


Figure 8. Physical diagram of deployment of wireless soil monitoring system. (a) Deploy TH30 sensors (b) Organize cables (c) Secure the data logger.

To verify the usability of the system, a pilot study of soil monitoring was carried out in the experimental field. The experiment was initiated on 14 June 2024 in the study area with data acquisition using the DL and soil sensors. Multiple TH30 soil sensors were arranged in the soil profile at different depths to obtain environmental data of the soil at each level and to simultaneously collect meteorological data, such as the air temperature and humidity. The system was set to send the measured values to the server every half hour, and the data were stored on the server for a long time and visualized through the soil monitoring cloud platform.

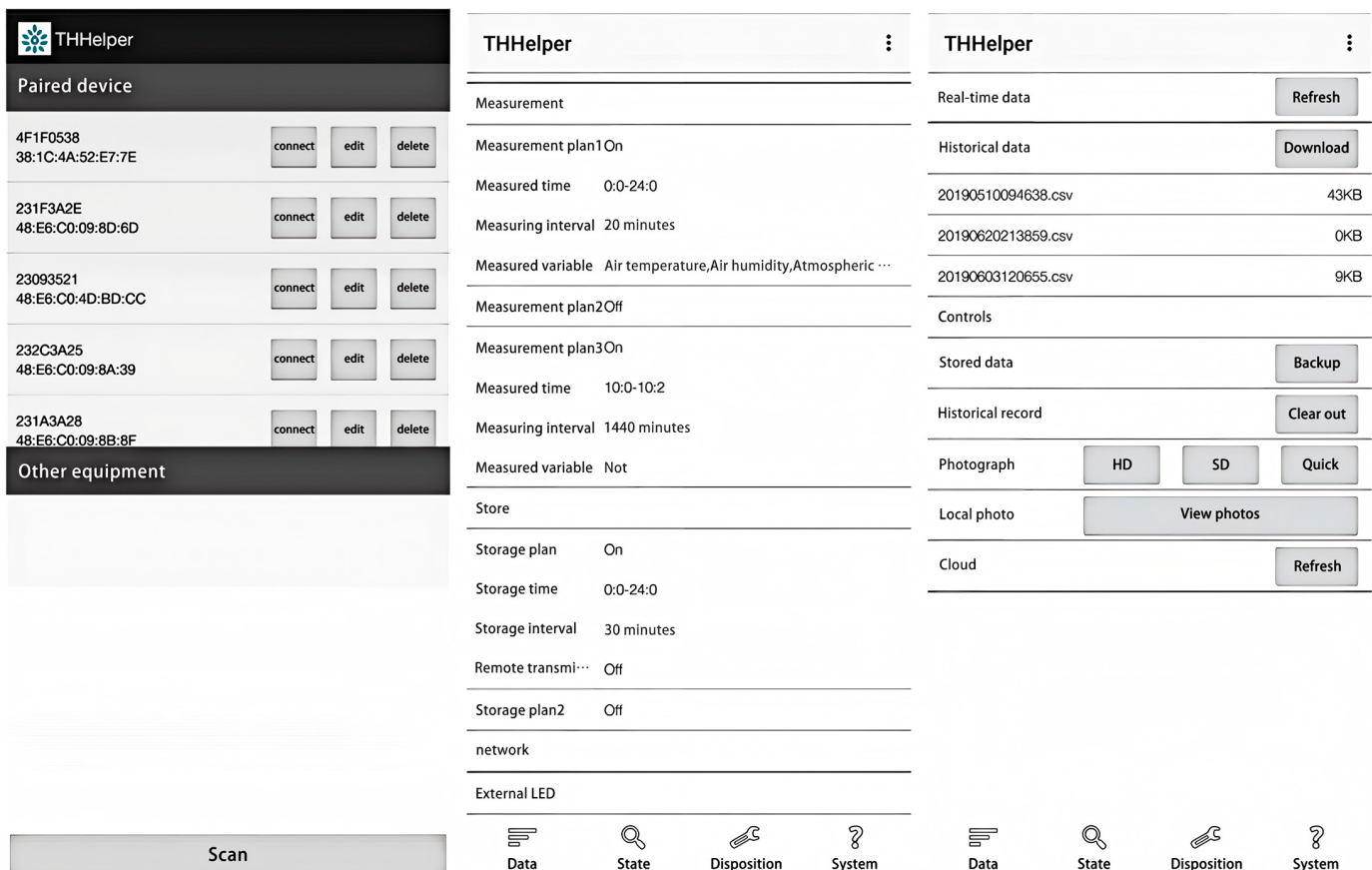


Figure 9. Mobile app interface.

2.3.2. Testing the Developed System

The experimental site was situated in Hebei, which is characterized by a typical arid climate. There is considerable temperature variation between the day and night, with an annual precipitation of merely 200–300 mm, accompanied by frequent gales (with the maximum wind speed reaching up to 20 m/s). The soil type of the experimental field is sandy loam, which possesses a relatively low water retention capacity. These environmental conditions simulate extreme agricultural production circumstances and can test the stability and reliability of the equipment under diverse climatic conditions. The experimental period of the system ranges from 14th June to 6th September 2024. This period encompasses sunny days, rainy days, and multiple instances of strong winds to ensure that the operating conditions of the system comprehensively cover various weather conditions. The battery voltage, the number of days of stable operation, and the missing rate of collected data were recorded to verify the stability and reliability of the system in extreme environments.

2.3.3. Model Construction and Testing

After obtaining a large amount of soil temperature and humidity monitoring data, this study adopted a machine learning model to predict soil moisture. In order to evaluate the performances of different machine learning models in soil moisture prediction, this study selected linear regression [36], decision trees [37], random forest [38], LSTM [39], and GBDTs [40] to construct soil moisture prediction models. The experimental process is as follows:

- (1) Data preprocessing: First, the raw data are cleaned, including the removal of noisy data and irrelevant features. In addition, the data are characterized to ensure their suitability for model training.

- (2) Feature selection: Based on domain knowledge, the atmospheric temperature and humidity, rainfall, and total solar radiation are selected as the input features of the model, while soil moisture is taken as the output. Additionally, time features are extracted from the dataset, such as the year, month, day, hour, minute, and second, to capture potential temporal patterns in the data. To enhance the diversity of the features and improve the model's ability to capture short-term trends and patterns of change, we introduce moving average features and sliding window difference features.
- (3) Model construction: Python's scikit-learn library is employed to develop individual models, including linear regression, decision trees, random forest, and GBDTs. Additionally, the LSTM model is implemented using PyTorch, leveraging its nn.LSTM module to capture temporal dependencies in sequential data. The architecture consists of a single LSTM layer followed by a fully connected layer to produce the final output. These models are further integrated to form a hybrid model–meta-model, combining their strengths to enhance prediction accuracy and robustness.
- (4) Data partitioning: Using the time-series split method, the dataset, comprising approximately 3800 data points, is partitioned into training, validation, and test sets in a 7:2:1 ratio. This approach aims to ensure the model's generalization capability on independent data.
- (5) Model hyperparameter optimization and training: First, the TPE hyperparameter optimization algorithm is employed to optimize the hyperparameters of each model. The models are then trained using the optimal hyperparameters. After training, the models are saved. The performances of the models are evaluated using the mean squared error (MSE), coefficient of determination (R^2), and root-mean-square error (RMSE).
- (6) Generalization ability analysis: The saved model is utilized to predict the test set data, thereby verifying the model's generalization ability. In this study, we focus on absolute error and relative error to evaluate the model's predictive performance. Consequently, we adopt the mean squared error (MSE) and root-mean-square error (RMSE) as evaluation metrics to provide a more intuitive and comprehensive assessment of prediction accuracy.

3. Experiments and Results

3.1. Experimental Results and Discussion

In the 84-day trial, the system demonstrated good stability and reliability: the power supply system performed stably, and the system adopted a design combining solar power and backup batteries to effectively ensure the continuity of energy supply. The battery voltage remained stable during the trial period, and no equipment downtime occurred due to insufficient power. The system ran stably for 80 days, with short interruptions of 4 days mainly caused by equipment failures rather than extreme weather conditions. However, the equipment was able to quickly resume operation after fault diagnosis and repair, indicating that the system design has strong maintainability and recovery capabilities. The data collection success rate was 95.87%, indicating that the system can maintain a high data transmission efficiency in the complex agricultural field environment. Although there were brief data gaps, the proportion was low, and the overall performance met the application requirements for agricultural environment monitoring.

A large amount of environmental data, such as the soil temperature, soil moisture at different depths, air temperature, and relative humidity, from the experimental field was collected through experiments. With the integration of Layui and ECharts technology, the dynamic visual display of data tables and charts was realized. The scheme significantly

improves the efficiency of data processing and analysis and provides more intuitive and efficient decision support for agricultural environmental monitoring.

The soil monitoring cloud platform is capable of visualizing the data of soil temperature and humidity as well as air temperature and humidity, as depicted in Figure 10. It offers intuitive soil parameter assessment tools for soil scientists and land managers and supports schema switching and downloading functions to facilitate users' saving and analysis. It promotes scientific decision making and the optimization of soil management.

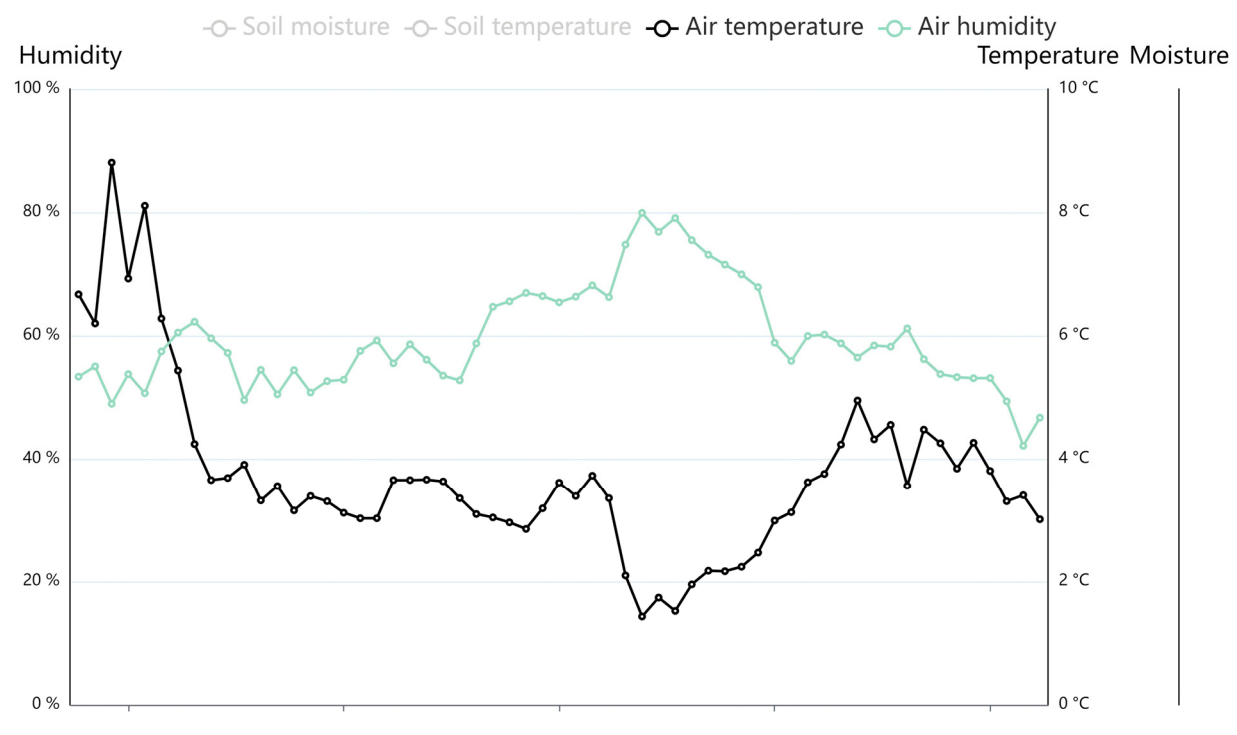
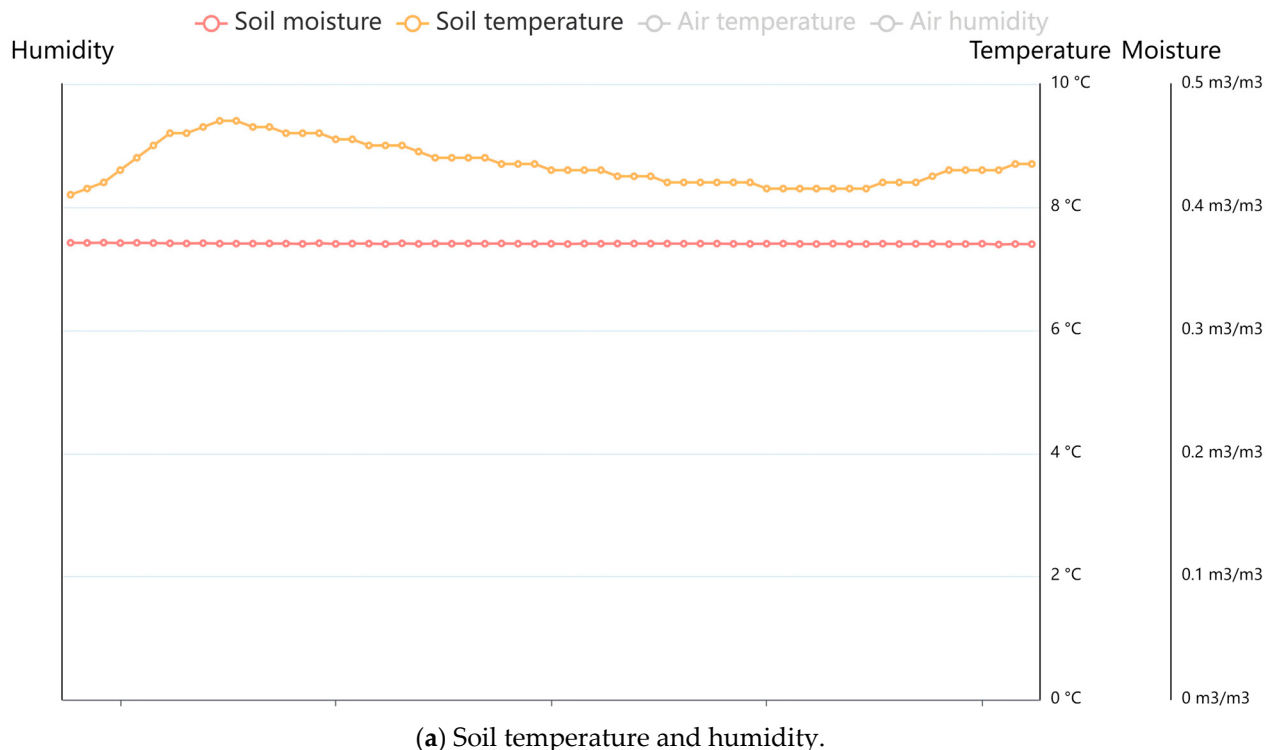


Figure 10. Cont.

Data table

start time yyyy-MM-dd HH:mm:ss
 endtime yyyy-MM-dd HH:mm:ss

1	2	3	4	5	6	7	8	9	10	11	12	13	14	15	16	17	18	19	20	21	22	23	24	25	26	27	28	29
Date	Data 1 (Soil Moisture)			Data 2 (Soil Temperature)			Data 3 (Air Temperature)			Data 4 (Air Humidity)																		
2024-08-26 19:00:00	0.3611372			27.2			27.770851			76.46895																		
2024-08-26 19:30:00	0.36091292			27.1			28.342232			75.0285																		
2024-08-26 20:00:00	0.36102512			26.9			27.306274			77.92008																		
2024-08-26 20:30:00	0.36091292			26.8			27.004562			78.63725																		
2024-08-26 21:00:00	0.3606884			26.7			28.069893			77.85294																		
2024-08-26 21:30:00	0.3606884			26.5			28.198051			77.67289																		
2024-08-26 22:00:00	0.36091292			26.4			28.04052			78.17949																		
2024-08-26 22:30:00	0.36091292			26.3			26.76159			81.79892																		
2024-08-26 23:00:00	0.3606884			26.2			27.83493			81.05581																		
2024-08-26 23:30:00	0.3603512			26.1			27.348991			81.45864																		
2024-08-27 00:00:00	0.3603512			26.0			27.47715			81.930145																		
2024-08-27 00:30:00	0.36046368			25.9			27.575943			82.23991																		

(c) Monitoring data form.

Figure 10. Visual chart of soil monitoring cloud platform.

Figure 11 shows the data of soil temperature and soil moisture at different depths (shallow (Mios1), middle (Mios2), and deep (Mios3) layers), as well as the air temperature and relative humidity of the experimental field. The following analysis focuses on data collected in August. Since rainfall in August is close to zero, it is not shown in the figure. However, affected by the availability of wet soil layers, water mainly concentrated in the soil surface, and the water content decreased significantly with the increase in soil depth. As can be seen from Figure 11, there is a positive correlation between air moisture and soil moisture, and the influence of air temperature on soil temperature is also positively correlated.

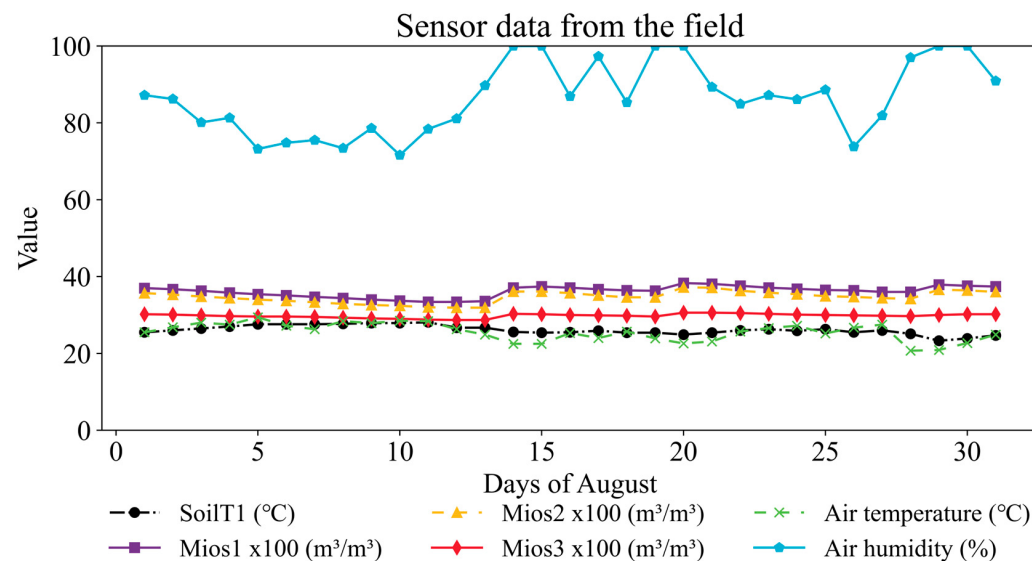


Figure 11. Soil data chart in August.

In summary, the functions of soil parameter measurement, data acquisition, data storage, and data visualization of the IoT system were successfully tested and verified, proving that the system is suitable for soil environmental monitoring and precision agriculture.

This study uses the collected data to build a soil moisture prediction model. The soil moisture prediction model can effectively assist the staff of the test station in analyzing and predicting the future soil moisture changes based on historical experience to provide a scientific basis for whether to implement irrigation measures.

3.2. Model Performance Assessment

3.2.1. Hyperparameter Optimization and Model Training

After hyperparameter optimization and training, we obtained the optimal hyperparameters for the six prediction models and generated comparison graphs of their prediction results against the validation set, as illustrated in Figure 12. The optimal hyperparameters for each model are detailed in Table 1, while the evaluation metrics are shown in Table 2.

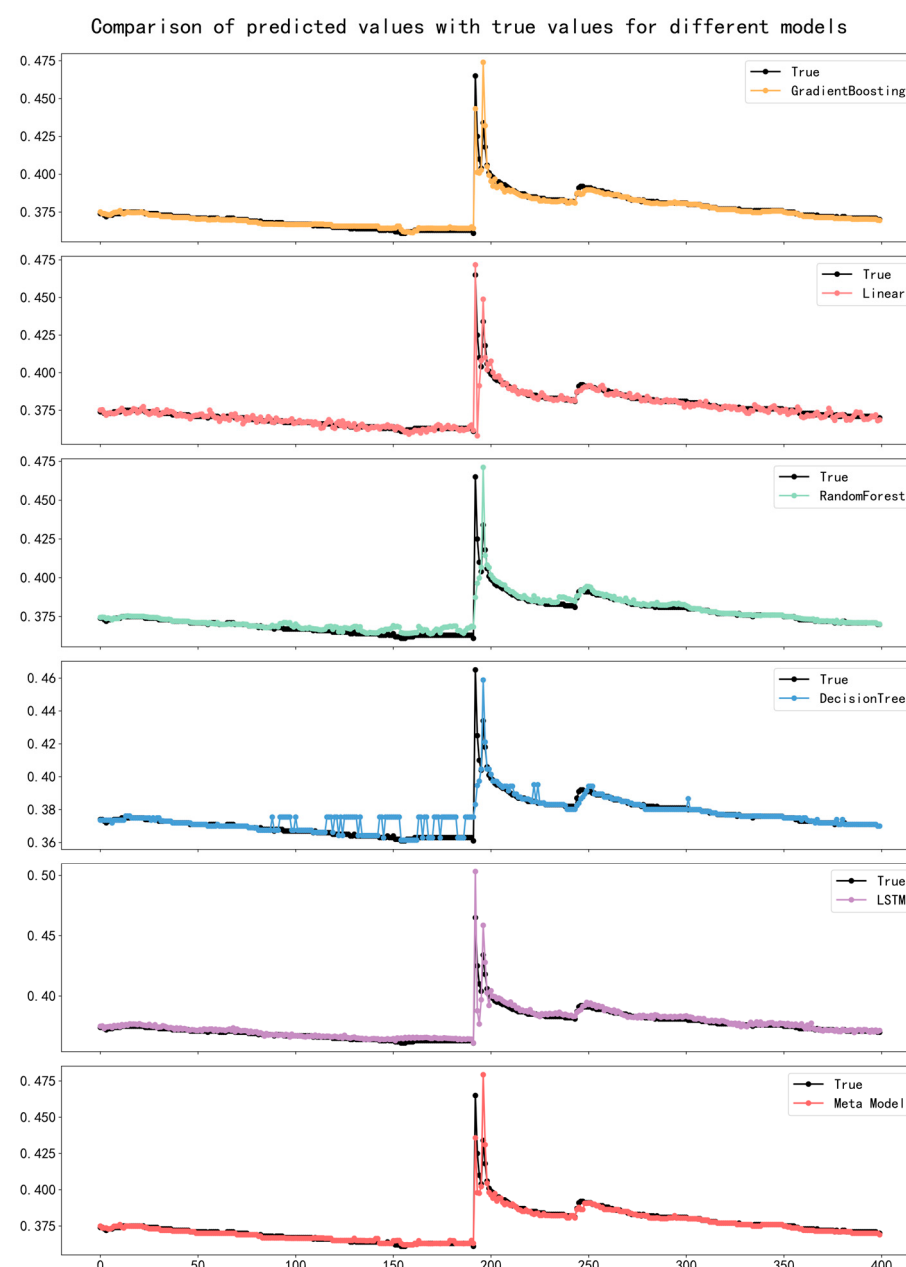


Figure 12. Comparison of prediction results of the six prediction models.

Table 1. The optimal hyperparameters of the five prediction models.

Model	Optimal Hyperparameters of the Model
Linear regression	'alpha': 0.00010000388939744078
Decision tree	'max_depth': 8, 'min_samples_split': 7, 'min_samples_leaf': 6
Random forest	'n_estimators': 296, 'max_depth': 27, 'min_samples_split': 2, 'min_samples_leaf': 5
LSTM	'hidden_size': 227, 'learning_rate': 0.004967542985882784, 'batch_size': 18
GBDT	'n_estimators': 150, 'learning_rate': 0.07622686624011799, 'max_depth': 3, 'subsample': 0.6000709412669746

Table 2. The evaluation metrics of the six models on the validation set (20%).

Model	Model Evaluation Coefficient		
	R ²	MSE (%)	RMSE (%)
Linear regression	0.9178	0.00090	0.30
Decision tree	0.8875	0.001225	0.35
Random forest	0.8578	0.001521	0.39
LSTM	0.8891	0.001156	0.34
GBDT	0.9838	0.0000169	0.13
Meta	0.9787	0.000196	0.14

As can be seen from Table 2, linear regression demonstrated strong predictive power, with an R² of 0.9178 and an RMSE of 0.0030, indicating a linear relationship between the features and soil moisture. However, due to its limited ability to capture nonlinear relationships, its performance was slightly inferior to that of ensemble methods. The decision tree and random forest models performed similarly, with R² values of 0.8875 and 0.8578, respectively. Although random forest should have outperformed the decision tree due to its ensemble nature, in this case, its performance was not significantly better, suggesting that further hyperparameter tuning or feature engineering might be necessary. The gradient boosting decision tree (GBDT) performed best, with an R² of 0.9838, an MSE of 0.00000169, and an RMSE of 0.0013. This result highlights its ability to effectively handle nonlinear patterns and interactions in the dataset. The meta-model, which combined multiple algorithms, performed nearly as well as the GBDT, with an R² of 0.9787 and a root-mean-square error of 0.0014. The LSTM model had an R² of 0.8891 and an RMSE of 0.0034, performing better than the decision tree and random forest models but still lagging behind the GBDT and meta-model. This might be due to insufficient feature engineering for time dependency and limited training data. The GBDT demonstrated excellent prediction accuracy and was the most suitable model in this study, although the meta-model achieved a comparable performance, showcasing its potential for integrating multiple algorithms to enhance accuracy. Traditional models like linear regression performed well but lacked flexibility in handling complex nonlinear relationships compared to ensemble methods. The meta-model showed strong potential as an alternative by combining multiple algorithms to enhance performance. The moderate performance of the LSTM model indicates the need for further optimization or more extensive time-series feature extraction.

While the evaluation metrics presented in Table 2 provide insights into the predictive accuracy of each model on the test dataset, it is equally important to assess their generalization ability when applied to unseen data. Generalization performance is critical for ensuring the robustness and reliability of predictions in practical applications.

3.2.2. Analysis of Model Generalization Ability

To evaluate the generalization performance of the model, we conducted prediction experiments on the test dataset using six trained models. The comparison between the

prediction results and the actual values in the test set is shown in Figure 13. The evaluation metrics are presented in Table 3.

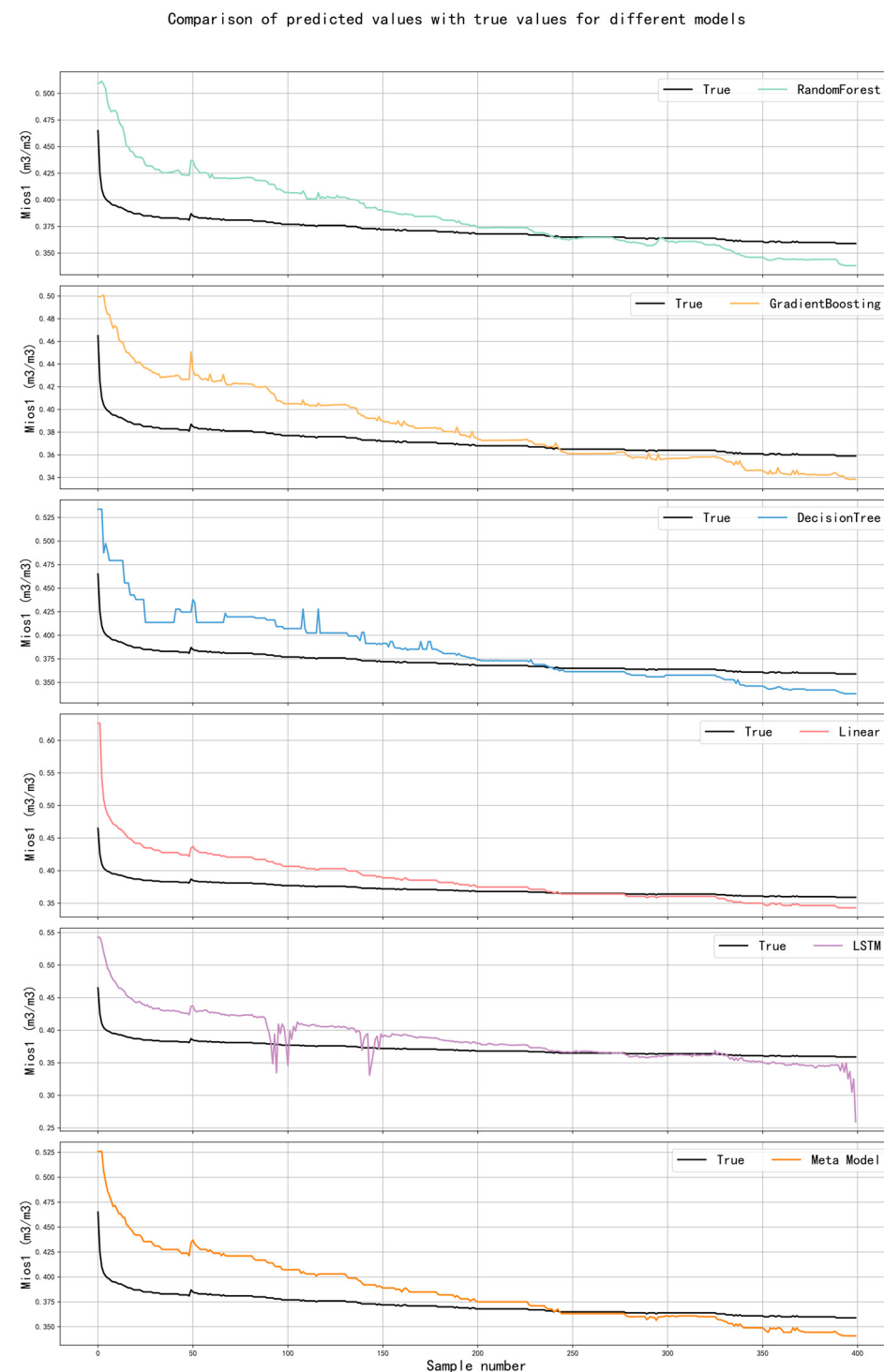


Figure 13. Comparison of prediction results of six models on the test set (10%).

As can be seen from Table 3, the decision tree model performed best on the test set, with a root-mean-square error (RMSE) of 0.0281 and a mean squared error (MSE) of 0.0008, indicating that it had the lowest prediction error among all models. The random forest and gradient boosting decision tree (GBDT) models performed comparably, with RMSEs of 0.0287 and 0.0285, respectively, and both had an MSE of 0.0008, showing stable performance. By contrast, the long short-term memory network (LSTM) and linear regression models

had higher prediction errors, with RMSEs of 0.0298 and 0.0308 and MSEs of 0.0009 and 0.0010, respectively. The prediction accuracy of these models was not as good as that of the others. Overall, in this experiment, the decision tree model outperformed the others, while ensemble methods such as random forest and the GBDT also demonstrated good performance.

Table 3. The evaluation metrics of the six models on the test set (10%).

Model	Model Evaluation Coefficient	
	RMSE (%)	MSE (%)
Linear regression	3.08	0.10
Decision tree	2.81	0.08
Random forest	2.87	0.08
LSTM	2.98	0.09
GBDT	2.85	0.08
Meta	2.85	0.08

Although all models have a relatively small RMSE and MSE on the test set, as shown in Figure 13, the fitting effect of the models to the actual values is not ideal. The main reasons can be attributed to the following points:

- (1) Insufficient data volume: During the training process, the lack of data may prevent the model from fully learning the underlying patterns in the data, especially in complex tasks where the model requires a sufficient number of samples to capture various variations and trends. Insufficient data may limit the model's generalization ability, resulting in poor fitting performance on the test set.
- (2) Insufficient data features: The current data features used may not fully reflect the complexity of soil moisture changes; especially, some key temporal features and environmental factors (such as seasonal variations and climatic conditions) have not been fully utilized. The insufficiency of feature engineering may prevent the model from comprehensively understanding the intrinsic relationships in the data, thereby affecting the prediction performance.
- (3) Overfitting or underfitting: Some models may have overfitting issues, meaning they perform well on the training set but fail to generalize effectively on the test set. This could be due to the model being overly complex and capturing noise in the training data. On the other hand, the model may also suffer from underfitting, where it is too simple to effectively capture the complex patterns in the data. Both overfitting and underfitting can lead to an unsatisfactory fitting effect.

3.2.3. Summary and Discussion of Model Performance

In conclusion, based on the performance of each model on both the validation and test sets, the GBDT model optimized via TPE hyperparameter tuning demonstrated superior performance in soil moisture prediction and is more suitable for agricultural environmental monitoring. The suboptimal performance of the LSTM model can be attributed to several factors, including high model complexity, insufficient data sample size, inadequate feature representation, and potential overfitting or underfitting. Through experiments and analysis, the following conclusions can be drawn:

- (1) In this study, the TPE algorithm was applied for hyperparameter optimization, and the R^2 of the GBDT model increased from 0.5879 to 0.9838, a rise of 67.34%, significantly enhancing the prediction accuracy of the GBDT model for soil moisture. Although traditional machine learning methods, such as linear regression, decision trees, and

random forest, have relatively low simulation accuracy, they remain feasible options for soil moisture prediction when the data volume is limited.

- (2) Different models are appropriate for distinct application scenarios and data characteristics. LSTM, as a deep learning model, excels in handling large datasets with rich feature sets. However, in this study, the limited data volume constrained its performance, preventing it from fully showcasing its potential. The ensemble method of meta-models demonstrated significant potential in this research. By integrating multiple algorithms, it enhanced prediction accuracy. Future research can further explore its applications.

4. Conclusions

This study developed an IoT-based wireless monitoring system for farmland soil to meet the demand for the continuous monitoring of farmland soil in actual agricultural production. The system achieves long-distance data transmission through Narrowband IoT (NB-IoT) wireless communication; integrates high-precision soil sensors, solar power supply modules, and GPS positioning modules; and can operate in extreme environments while providing high-precision parameters. The system was deployed and tested at an agricultural experimental station for 84 days, and its performance in soil detection, equipment power consumption, and implementation cost was evaluated. The test results showed that the system operated stably for 80 days, with a data collection success rate of 95.87%, indicating good stability and reliability. In addition, the system's visual interface enhances data readability, making the decision-making process more intuitive. The cost is lower than that of existing soil monitoring systems at home and abroad, and the system has high precision, a wide range of monitoring parameters, and a long working life.

This system also has the function of parameter prediction. Taking soil moisture as an example, using the collected experimental data and combining the method of hyperparameter optimization, a soil moisture prediction model was constructed, and its generalization ability was analyzed. The experimental results showed that the GBDT model performed the best, with model training evaluation indicators of $R^2 = 0.9838$, $RMSE = 0.013$, and $MSE = 0.00000169$ and generalization ability analysis evaluation indicators of $RMSE = 0.0285$ and $MSE = 0.0008$. The GBDT model can predict future soil moisture data well.

Future research will focus on further expanding the types of sensors; expanding the equipment layout area; introducing more features, such as the soil pH value, vegetation index (NDVI), atmospheric pressure, and other environmental factors; and exploring more complex soil moisture prediction relationships. This not only increases the data dimension but also helps improve the prediction accuracy of the model. Also, more complex models can be used to further improve prediction accuracy and generalization ability. With more data support, WebGIS functions will be developed, map service functions will be optimized, and the distribution of soil parameter heat maps will be realized to achieve wider applications.

Author Contributions: Funding acquisition, S.Z. and Y.H.; project administration, S.Z.; resources, Y.H.; software, G.O. and Y.S.; visualization, G.O.; writing—original draft preparation, G.O.; writing—review and editing, Y.C. and R.M. All authors have read and agreed to the published version of the manuscript.

Funding: This study was financially supported by the Rural Energy and Environment Agency, Ministry of Agriculture and Rural Affairs Fund Program, the National Key Research and Development Program (Grant No. 2021YFD2000205), and the Modern agricultural industrial Technology System construction special fund project (Grant No. CARS-24-B-05).

Institutional Review Board Statement: Not applicable.

Data Availability Statement: The data presented in this study contain sensitive information relating to the Rural Energy and Environment Agency, Ministry of Agriculture and Rural Affairs. No information is allowed to be used without the prior consent of the Rural Energy and Environment Agency, Ministry of Agriculture and Rural Affairs.

Acknowledgments: The authors are grateful for the support of the Rural Energy and Environment Agency, Ministry of Agriculture and Rural Affairs.

Conflicts of Interest: The authors declare no conflicts of interest.

References

1. Ojha, T.; Misra, S.; Raghuvanshi, N.S. Wireless sensor networks for agriculture: The state-of-the-art in practice and future challenges. *Comput. Electron. Agric.* **2015**, *118*, 66–84. [[CrossRef](#)]
2. Jangam, A.R.; Kale, K.V.; Gaikwad, S.; Vibhute, A.D. Design and Development of IoT based System for Retrieval of Agrometeorological Parameters. In Proceedings of the International Conference on Recent Innovations in Electrical, Electronics and Communication Engineering, Bhubaneswar, India, 27–28 July 2018.
3. Ayaz, M.; Ammad-Uddin, M.; Sharif, Z.; Mansour, A.; Aggoune, E.H. Internet-of-Things (IoT)-Based Smart Agriculture: Toward Making the Fields Talk. *IEEE Access* **2019**, *7*, 129551–129583. [[CrossRef](#)]
4. Elijah, O.; Rahman, T.A.; Orikumhi, I.; Leow, C.Y.; Hindia, M.N. An Overview of Internet of Things (IoT) and Data Analytics in Agriculture: Benefits and Challenges. *IEEE Internet Things J.* **2018**, *5*, 3758–3773. [[CrossRef](#)]
5. Antonopoulou, E.; Karetos, S.; Maliappis, M.; Sideridis, A. Web and mobile technologies in a prototype DSS for major field crops. *Comput. Electron. Agric.* **2010**, *70*, 292–301. [[CrossRef](#)]
6. Fountas, S.; Carli, G.; Sørensen, C.G.; Tsiropoulos, Z.; Cavalaris, C.; Vatsanidou, A.; Liakos, B.; Canavari, M.; Wiebensohn, J.; Tisserye, B.A. Farm management information systems: Current situation and future perspectives. *Comput. Electron. Agric.* **2015**, *115*, 40–50. [[CrossRef](#)]
7. Nabi, F.; Jamwal, S.; Padmanabh, K. Wireless sensor network in precision farming for forecasting and monitoring of apple disease: A survey. *Int. J. Inf. Technol.* **2020**, *14*, 769–780. [[CrossRef](#)]
8. Rossel, R.V.; McBratney, A.B. Laboratory evaluation of a proximal sensing technique for simultaneous measurement of soil clay and water content. *Geoderma* **1998**, *85*, 19–39. [[CrossRef](#)]
9. Kashyap, B.; Kumar, R. Sensing Methodologies in Agriculture for Soil Moisture and Nutrient Monitoring. *IEEE Access* **2021**, *9*, 14095–14121. [[CrossRef](#)]
10. Futagawa, M.; Iwasaki, T.; Murata, H.; Ishida, M.; Sawada, K. A Miniature Integrated Multimodal Sensor for Measuring pH, EC and Temperature for Precision Agriculture. *Sensors* **2012**, *12*, 8338–8354. [[CrossRef](#)] [[PubMed](#)]
11. Ramson, S.J.; Vishnu, S.; Shanmugam, M. Applications of Internet of Things (IoT)—An Overview. In Proceedings of the 2020 5th International Conference on Devices, Circuits and Systems (ICDCS), Coimbatore, India, 5–6 March 2020.
12. Pathinarupothi, R.K.; Durga, P.; Rangan, E.S. IoT-Based Smart Edge for Global Health: Remote Monitoring with Severity Detection and Alerts Transmission. *IEEE Internet Things J.* **2018**, *6*, 2449–2462. [[CrossRef](#)]
13. Fortino, G.; Russo, W.; Savaglio, C.; Viroli, M.; Zhou, M. Modeling Opportunistic IoT Services in Open IoT Ecosystems. *WOA* **2017**, 90–95.
14. Kuang, B.; Mahmood, H.S.; Quraishi, M.Z.; Hoogmoed, W.B.; Mouazen, A.M.; van Henten, E.J. Sensing Soil Properties in the Laboratory, In Situ, and On-Line. *Adv. Agron.* **2012**, *114*, 155–224.
15. Ramson, S.J.; Moni, D.J. Wireless sensor networks based smart bin. *Comput. Electr. Eng.* **2017**, *64*, 337–353, S0045790616309065. [[CrossRef](#)]
16. Madhura, U.; Akshay, P.; Bhattacharjee, A.J.; Nagaraja, G. Soil Quality Management Using Wireless Sensor Network. 2018. In Proceedings of the 2017 2nd International Conference on Computational Systems and Information Technology for Sustainable Solution (CSITSS), Bengaluru, India, 21–23 December 2017.
17. Villalba, G.; Plaza, F.; Zhong, X.; Davis, T.W.; Navarro, M.; Li, Y.; Slater, T.A.; Liang, Y.; Liang, X. A Networked Sensor System for the Analysis of Plot-Scale Hydrology. *Sensors* **2017**, *17*, 636. [[CrossRef](#)]
18. Estrada-López, J.J.; Castillo-Atoche, A.A.; Vázquez-Castillo, J.; Sánchez-Sinencio, E. Smart Soil Parameters Estimation System Using an Autonomous Wireless Sensor Network with Dynamic Power Management Strategy. *IEEE Sens. J.* **2018**, *19*, 8913–8923. [[CrossRef](#)]
19. Roy, A.; Barman, K. An Adaptive Technique For Soil Moister Control and Nutrient Monitoring Using Wireless Sensor Network. *Think India J.* **2019**, *22*, 1558–1564.

20. Vieira, R.G.; Da Cunha, A.M.; Ruiz, L.B.; De Camargo, A. On the Design of a Long Range WSN for Precision Irrigation. *IEEE Sens. J.* **2017**, *18*, 773–780. [[CrossRef](#)]
21. Kuang, Y.; Shen, Y.; Lu, L.; Li, G. Farmland Monitoring System Based on Cloud Platform. In Proceedings of the 2019 IEEE 8th Joint International Information Technology and Artificial Intelligence Conference (ITAIC), Chongqing, China, 24–26 May 2019.
22. Rachmani, A.F.; Zulkifli, F.Y. Design of IoT Monitoring System Based on LoRa Technology for Starfruit Plantation. In Proceedings of the TENCON 2018-2018 IEEE Region 10 Conference, Jeju Island, Republic of Korea, 28–31 October 2018.
23. Davcev, D.; Mitreski, K.; Trajkovic, S.; Nikolovski, V.; Koteli, N. IoT agriculture system based on LoRaWAN. In Proceedings of the 2018 14 th IEEE International Workshop on Factory Communication Systems (WFCS), Imperia, Italy, 13–15 June 2018; pp. 1–4.
24. Gia, T.N.; Qingqing, L.; Queralta, J.P.; Zou, Z.; Tenhunen, H.; Westerlund, T. Edge AI in Smart Farming IoT: CNNs at the Edge and Fog Computing with LoRa. In Proceedings of the 2019 IEEE AFRICON, Accra, Ghana, 25–27 September 2019.
25. Bishop, M.P.; James, L.A.; Shroder, J.F., Jr.; Walsh, S.J. Geospatial technologies and digital geomorphological mapping: Concepts, issues and research. *Geomorphology* **2012**, *137*, 5–26. [[CrossRef](#)]
26. Alrajeh, N.A.; Bashir, M.; Shams, B. Localization Techniques in Wireless Sensor Networks. *Int. J. Distrib. Sens. Netw.* **2013**, *9*, 304628. [[CrossRef](#)]
27. Gaikwad, S.V.; Vibhute, A.D.; Kale, K.V.; Nalawade, D.B.; Jadhav, M.B. Design and Development of Ground Truth Collection Platform Using Android and Leaflet Library. In Proceedings of the Recent Trends in Image Processing and Pattern Recognition: Second International Conference, Solapur, India, 21–22 December 2018.
28. Sawant, S.; Durbha, S.S.; Jagarlapudi, A. Interoperable agro-meteorological observation and analysis platform for precision agriculture: A case study in citrus crop water requirement estimation—ScienceDirect. *Comput. Electron. Agric.* **2017**, *138*, 175–187. [[CrossRef](#)]
29. Ramadan, K.M.; Oates, M.J.; Molina-Martinez, J.M.; Ruiz-Canales, A. Design and implementation of a low cost photovoltaic soil moisture monitoring station for irrigation scheduling with different frequency domain analysis probe structures. *Comput. Electron. Agric.* **2017**, *148*, 148–159. [[CrossRef](#)]
30. Mesas-Carrascosa, F.J.; Santano, D.V.; Meroño, J.E.; De La Orden, M.S.; García-Ferrer, A. Open source hardware to monitor environmental parameters in precision agriculture. *Biosyst. Eng.* **2015**, *137*, 73–83. [[CrossRef](#)]
31. Cui, L.; Yang, S.; Chen, F.; Ming, Z.; Lu, N.; Qin, J. A survey on application of machine learning for Internet of Things. *Int. J. Mach. Learn. Cybern.* **2018**, *9*, 1399–1417. [[CrossRef](#)]
32. Shokati, H.; Mashal, M.; Noroozi, A.; Abkar, A.A.; Mirzaei, S.; Mohammadi-Doqozloo, Z.; Taghizadeh-Mehrjardi, R.; Khosravani, P.; Nabiollahi, K.; Scholten, T. Random Forest-Based Soil Moisture Estimation Using Sentinel-2, Landsat-8/9, and UAV-Based Hyperspectral Data. *Remote Sens.* **2024**, *16*, 1962. [[CrossRef](#)]
33. Wang, Y.; Shi, L.; Hu, Y.; Hu, X.; Song, W.; Wang, L. A comprehensive study of deep learning for soil moisture prediction. *Hydrol. Earth Syst. Sci. Discuss.* **2024**, *28*, 917–943. [[CrossRef](#)]
34. Li, D.; Mei, H.; Shen, Y.; Su, S.; Zhang, W.; Wang, J.; Zu, M.; Chen, W. ECharts: A declarative framework for rapid construction of web-based visualization. *Vis. Inform.* **2018**, *2*, 11. [[CrossRef](#)]
35. Suryotrisongko, H.; Jayanto, D.P.; Tjahyanto, A. Design and Development of Backend Application for Public Complaint Systems Using Microservice Spring Boot. *Procedia Comput. Sci.* **2017**, *124*, 736–743. [[CrossRef](#)]
36. Draper, N.R. Applied regression analysis. *Technometrics* **1998**, *9*, 182–183.
37. Quinlan, J.R. Induction of decision trees Machine Learning. *Mach. Mediat. Learn.* **1986**, *1*, 81–106. [[CrossRef](#)]
38. Breiman, L. Random forests. In *Machine Learning*; Springer: Berlin/Heidelberg, Germany, 2001; Volume 45, pp. 5–32.
39. Hochreiter, S.; Schmidhuber, J. Long Short-Term Memory. *Neural Comput.* **1997**, *9*, 1735–1780. [[CrossRef](#)]
40. Friedman, J.H. Greedy Function Approximation: A Gradient Boosting Machine. *Ann. Stat.* **2001**, *29*, 1189–1232. [[CrossRef](#)]

Disclaimer/Publisher’s Note: The statements, opinions and data contained in all publications are solely those of the individual author(s) and contributor(s) and not of MDPI and/or the editor(s). MDPI and/or the editor(s) disclaim responsibility for any injury to people or property resulting from any ideas, methods, instructions or products referred to in the content.